A PHOTOMETRIC INVESTIGATION OF THE LUNAR CRATER RAYS

J. VAN DIGGELEN

The Astronomical Institute, University of Utrecht, Holland

(Received 7 July, 1969)

Abstract. This investigation deals with accurate photometric data concerning a number of rays of Tycho, Copernicus, Kepler, and Aristarchus. They have been derived from plates taken at the Yerkes Observatory in a night of a total lunar eclipse near phase angle 0°. By comparing the normal albedo with that of the surroundings of the rays we found that they can be interpreted as samples of telescopically unresolved bright patches. The fractional area k covered by these patches varies along the ray and shows that they are composed of a number of separate ray elements. The observed value of k is in accordance with counts on a Ranger photograph.

The distribution of the brightness along the rays has also been compared with the mass distribution of the ejecta in the rays around terrestrial explosion craters. The mean length of the lunar rays is in full accordance with its extrapolated terrestrial value. We cannot assume, however, that the rays are regions covered with a homogeneous layer of white powder, because the comparison with the terrestrial explosion craters gives an unprobable value for the height of the layer of the ejecta. The same results follow now from the photometric properties of the rays.

From a comparison with the difference in albedo at the Surveyor's footprints follows the suggestion that the lunar rays are composed of bright patches, where the surface material came into a state of lower porosity, while it has a higher porosity in the dark halos around the craters. A suspected dark halo around Tycho has photometrically been measured and the results prove that it really exists. Kepler also shows a very weak halo.

1. The Nature of the Ray Systems

A curious characteristic of many lunar craters is a system of bright rays. These rays appear as permanent markings showing like white streaks which cross the lunar surface. The rays of such a system diverge from its central crater along great circles which intersect at the centre of the crater. Some rays, however, appear to originate in the walls of the crater rather than in its centre or come form outside the wall. There is no doubt that the ray systems are connected with the craters from which they diverge.

The rays do not always follow great circles. Two types of rays are usually distinguished, the Tycho and the Copernicus type. Tycho has the largest ray aureole known on the Moon, Copernicus the second largest. The rays of Tycho (Figure 1) are long and straight and some extend over 1000 km or more. They are more coherent than the Copernicus type rays and are also much brighter. The Kepler rays conform in structure to the Tycho kind, those of Copernicus (Figure 2), however, do not. This system consists mainly of arc-like and loop-shaped streaks.

Visual investigation and photographs with large telescopes have shown that both types of rays are composed of linear or feather-shaped elements, ranging from 15 to 50 km in length. The rays extend up to distances which are often of the order of 10 crater diameters. The position of their end points cannot be determined accurately.

The rays have no perceptible thickness and cast no observable shadows. They are not deviated by mountains, ridges or other features which they all cross over and only occasionally 'shadow zones' may be found behind prominent elevations (Fielder, 1965). They show as superficial features, but they behave in the same way as the regions through which they pass. The brightness of the rays show that they consist of relatively highly reflective material on a generally darker part of the Moon's surface. The photometric properties of the bright rays and those of neighbouring darker regions coincide.

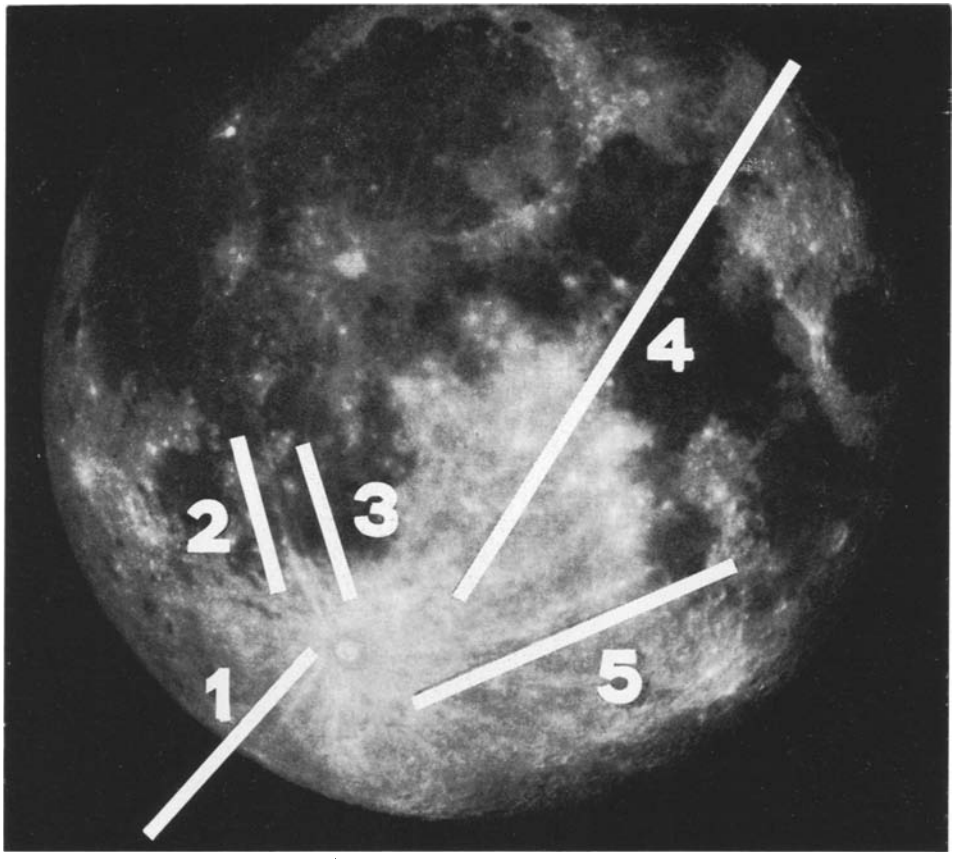

Fig. 1. Rays 1–5 of Tycho.

The formation of these bright rays and aureoles must be the result of some kind of explosive phenomenon related with the origin of its central crater. Many astronomers suppose that they are formed by powdery matter ejected from the central crater and spread over a previously existing surface. Photometric data should support the reality of this hypothesis. The normal albedo of a ray may contain the integrated

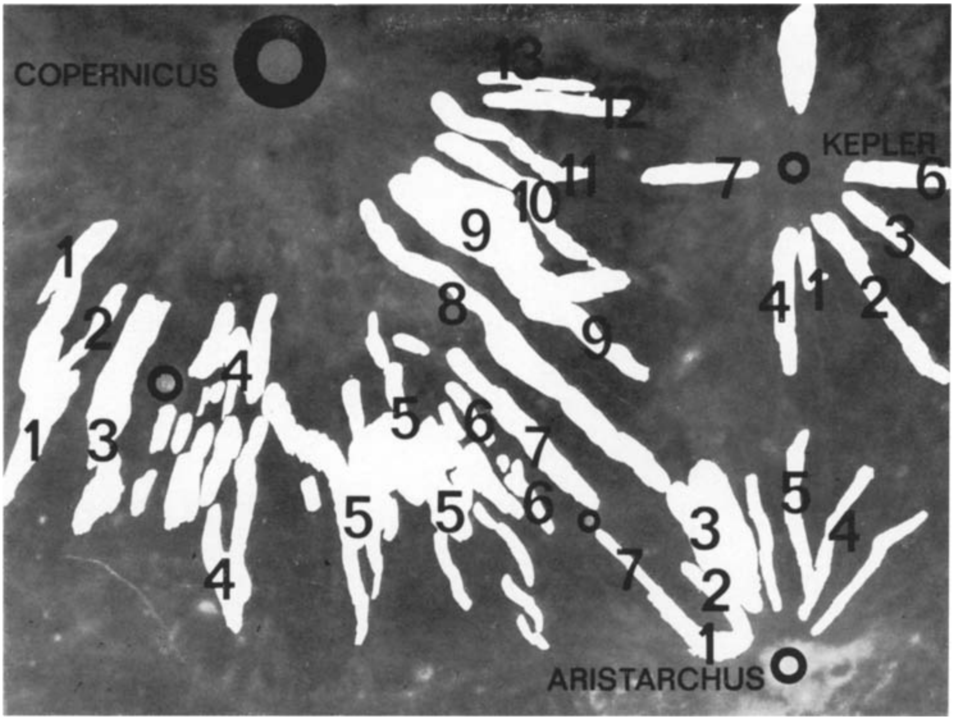

Fig. 2. Rays 1–13 of Copernicus, 1–5 of Aristarchus, and 1–7 of Kepler.

effect of the ejected powder and the lunar material which was locally present at the lunar surface before the rays were formed. New accurate photometric data may be of great interest, as we do not know much about the origin of these craters and their rays.

2. Photometry of the Rays

The first, who listed some photometric measurements on individual rays was Graff (1948). He has given data on 5 rays of Tycho. Visual and photographic measurements of the colour of three of the brightest rays of Tycho, three rays of Copernicus, and two rays originating from Kepler have been carried out by Radlova (1943).

In this investigation we give new and more accurate photometric data of a number of rays of Tycho, Copernicus, Kepler, and Aristarchus. They have been derived from plates taken at the Yerkes Observatory by G. P. Kuiper and A. Lenham during the night of November 19, 1956. In this night a total eclipse of the Moon enabled them to photograph the Moon near phase-angle $g=0°$ (values of $0°.7<g<1°.3$ have been obtained). The data of the plates have been published elsewhere (Van Diggelen, 1965).

On some of the plates we investigated the radiance of a number of rays (Tables I–IV). The transmission was measured with the Utrecht Observatory microphotometer. Each ray was measured along *AA*, *BB*, *CC*, ... (Figure 3) at regular intervals.

TABLE I

Normal albedo (ϱ) of five Tycho rays compared with the normal albedo of the background (ϱ_p), both $\times 10^3$. D = distance to the center of Tycho. G = observation of Graff (1948)

Ray 1			Ray 2			Ray 3			Ray 4			Ray 5		
D (km)	ϱ	ϱ_p	D (km)	ϱ	ϱ_p	D (km)	ϱ	ϱ_p	D (km)	ϱ	ϱ_p	D (km)	ϱ	ϱ_p
65		118	75	115		75		113	55		115	70	137	125
125	134	114	100	130	121	100		120	65		121	105		129
150	128	G	125	139	125	125	128	122	80		123	140	145	133
165	128	114	150	139	126	150	138	129	160		132	175	153	142
200	130	110	175	140	132	175	141	132	215	150	126	210	161	137
240	109	107	200	147	129	200	146	127	270		128	245	161	141
280	130	113	225	141		225	136	125	325	129	115	280	157	145
330	131	111	250	140	115	250	139	115	380		107	370	145	127
385	127	108	275	137	115	270	149	138	435	123	107	405	142	125
430	129	G	290	140	113	290	136		490	109	102	440	142	124
435	124	107	300	146	G	300	129	G	545	126	105	460	135	G
485	128	106	310	140	112	310	143	120	580	142	G	510	136	120
545	116	104	325	135	110	335	143	120	600	125	110	545	137	114
595	126	112	350	142	115	350	131	113	655		99	615	124	109
640	120	G	360	149	G	365	141	G	710	110	104	650	122	190
645	113	109	370	150	123	370	134	112	765	137	106	670	133	G
710	120	111	390		110	390	139	110	820	117	104	680	141	124
790	123	114	410	140	106	410	125	105	850	121	G	720	139	123
860	128	113	430	142	110	430		110	875	105	102	755	145	106
940	114	103	450	142	101	450	106	96	930	116	102	790	145	106
			460	139	G	460	126	G	985	134	106	825	130	102
			470	131	100	470	110	89	1000	127	G	860		106
			490	117	91	490	108	79	1040	122	103	895	131	107
			510	139	85	510	103	75	1085	123	111	930	129	108
			515	127	G	530	94	73	1140	140	117	940	121	G
			530	117	84	550	91	73	1150	130	G	965	134	111
			550	106	80	570	96	72	1190	122	110	1000	130	111
			570	106	82	590	91	72	1235	119	108	1040	134	106
			590	97	63	605	103	G	1290		105	1070	118	105
			610	106	G	610	96		1340	119	101	1110	117	107
			615	102	68	630	83	72	1395	121	109	1115	117	G
			630	102	72	650	99		1440	136	110	1150	109	91
			650	109	74	670	107		1490	138	112	1190	102	86
			670	99	75	685		75	1540	127	103	1230	93	85
			690	93	80	730		81	1590	138	102	1270	93	86
			710	93	74	735	93	G	1640	102	89	1310	105	85
			730	93	80	745		79	1680	103	78	1350	108	92
			750	96	G	770		80	1730	102	71	1390	116	98
			760	103	81	790		80	1775	107	71	1430	116	106
			770	99		805	88		1790	99	G			
			780	103	82	830	93	79	1805	97	72	1470	145	116
			800	98	80	840	113	78	1950		77	1510	139	103
			820	121	88	865	111	77	2000	81	76	1640	116	91
			840	115	87	885	110		2100	86	73	1670	94	83
			860	105	87	900	116		2200	85	83	1710		82
			880	111	66	920	100	76	2300	85	77	1750	84	78
			900	112	68	940	107	73	2400	82	72	1790		83
			920	121	76	965		73	2500	81	71			
			940	104	73	970	86	73	2550	101	90			

Table I (continued)

Ray 1			Ray 2			Ray 3			Ray 4			Ray 5		
D (km)	ϱ	ϱ_p	D (km)	ϱ	ϱ_p	D (km)	ϱ	ϱ_p	D (km)	ϱ	ϱ_p	D (km)	ϱ	ϱ_p
			960	90	72	1000	81	77	2605	91	74			
			970	96	G	1040		79	2720	77	69			
			980	96	73	1060	83	77	2805	131	96			
			1000	94	76	1110		75	2905	127	97			
			1020	99					3020	127	86			
			1040	104	78				3150	119	99			
			1060	101	77				3270		122			
			1080	91	81				3401	145	121			
									3560		110			

TABLE II

Normal albedo (ϱ) of 13 rays of Copernicus compared with the normal albedo of the background (ϱ_p), both $\times 10^3$. D = distance to the center of Copernicus

Ray 1			Ray 2			Ray 3			Ray 4			Ray 5		
D (km)	ϱ	ϱ_p	D (km)	ϱ	ϱ_p	D (km)	ϱ	ϱ_p	D (km)	ϱ	ϱ_p	D (km)	ϱ	ϱ_p
220	131	125	190	131	129	150	140	119	160		153	280	129	100
240	139	119	205	129	121	170	134	121	180		148	300	113	110
260	134	114	240	119	110	210	129	111	190	145		320	119	106
280	127	112	255	131	110	235	121	110	200		138	340	110	90
295	130	112	275	119	108	255	132	110	210	142	138	360	119	88
315	121	108	290	111	105	275	134	109	230	142	111	380	99	86
340	126	105	315	112	107	295	121	106	260	127		400	97	90
355	123	103	330	113	103	315	128	105	280	133	100	420	104	86
370	125	110				335	129	106	290	133	110	440	96	86
390	122	106				350	125	106	320		106	460	103	84
415	117	108				370	132	106	350	106	90	480	94	84
470	117	104				415	119	106	370	110	84	500	94	82
490	133	100				430	119	103	390	108	89	530	94	80
510	126	102				450	125	102	410	102	86			
530	119	106				465	114	106	430	97	86			
550	122	106				490	114	106	450	96	80			
570	125	106				510	114	101	470	101	85			
590	130	103				530	112	104	495	101	81			
610	140	108				550	120	111	530	111	80			
630	132	110				570	121	114	560		83			
650	121	104												

Ray 6			Ray 7			Ray 8			Ray 9			Ray 10		
D (km)	ϱ	ϱ_p	D (km)	ϱ	ϱ_p	D (km)	ϱ	ϱ_p	D (km)	ϱ	ϱ_p	D (km)	ϱ	ϱ_p
290	131	110	160		153	160		153	150	176		290		110
310	111	104	180		148	180	158	148	160		163	310	135	
330	111	102	200		138	200	138		175	170	148	320		106
350	128	90	230	133	111	225	138		200	163	138	330	128	
370	119	84	255	131	124	240	156	111	210		138	340		89
390	122	89	280	138	110	260	129	125	225	145		355	115	

Table II (continued)

Ray 6

D (km)	Q	Q_p
405	118	85
430	99	86
450	114	80
470	96	85
490	93	82
510	93	81
540	86	80

Ray 7

D (km)	Q	Q_p
305	114	
320		106
330	114	
340		90
355	115	
360		88
370		84
380	122	
390		89
410	110	
420		86
430	110	
440		86
450		81
470		84
480	91	
495		81
505	91	
515		81
530	89	
540		80
555	84	84
580	93	

Ray 8

D (km)	Q	Q_p
280		100
285	135	110
305	113	
320		106
330	111	
340		90
360	104	88
370		84
390	103	90
420	108	86
440		86
450	115	80
470		84
480	106	84
495		81
515		80
520	101	
540		80
555		83

Ray 9

D (km)	Q	Q_p
235		111
250	145	
255		125
275	152	
280		100
290		110
300	135	
320		106
340		90
350	123	
360		88
370		84
390		90
400	115	
420		86
425	104	
440		86
450	110	80
470		85
475	104	84
495		81
500	93	
510		80
525	96	
540		80
555		83

Ray 10

D (km)	Q	Q_p
360		88
380		84
385	119	
390		89
415	111	86
440		86
450	104	80
470		84
480		83

Ray 11

D (km)	Q	Q_p
160		153
175	172	
180		148
195	165	
200		138
215	153	138
230		111
240	150	
260		124
275	140	
280		100
290		110
310	115	
315		106
340		89

Ray 12

D (km)	Q	Q_p
100	129	90
110	132	90
120	134	90
145	133	90
155	129	90
170	125	90
180	125	90
190	115	90
200	118	90
215	118	90
225	117	90
235	117	90
250	117	90
260	111	90
270	106	90
280	103	90
295	99	90
305	97	90
315	93	90
325	90	90

Ray 13

D (km)	Q	Q_p
100	138	90
120	134	90
135	125	90
150	129	90
155	131	90
170	129	90
180	122	90
190	118	90
200	117	90
215	108	90
225	106	90
235	100	90
245	98	90
260	96	90
270	90	90

TABLE III

Normal albedo (ϱ) of 5 rays of Aristarchus compared with the normal albedo of the background (ϱ_p), both $\times 10^3$. D = distance to the center of Aristarchus

Ray 1			Ray 2			Ray 3			Ray 4			Ray 5		
D (km)	ϱ	ϱ_p	D (km)	ϱ	ϱ_p	D (km)	ϱ	ϱ_p	D (km)	ϱ	ϱ_p	D (km)	ϱ	ϱ_p
180	105	91	70	114	97	130	106	81	95	100	88	160	98	86
205	91	87	85	100	88	150	103	81	110	100	92	180	89	81
230	98	81	100	100	92	170	96	84	130	98	86	200	90	81
255	86	81	125	102	86	190	113	84	150	98	81	225	92	79
280	91	79	150	103	81	215	110	81	175	101	81	250	97	
305	94		175	100	81	235	115	86	200	91	79	275	117	82
330	94	81	200	94	79	270	111	87	225	97		300	101	85
			225	90		290	113	82	250	109	82	350	109	
			250	95	82	310	111	85	275	98	86	325	108	90
						330	115	90	300	111	90	375	106	86
						350	117	89	325	102		400	102	89
						370	106	90	350	98	87			
						395	99	98	375	106	89			

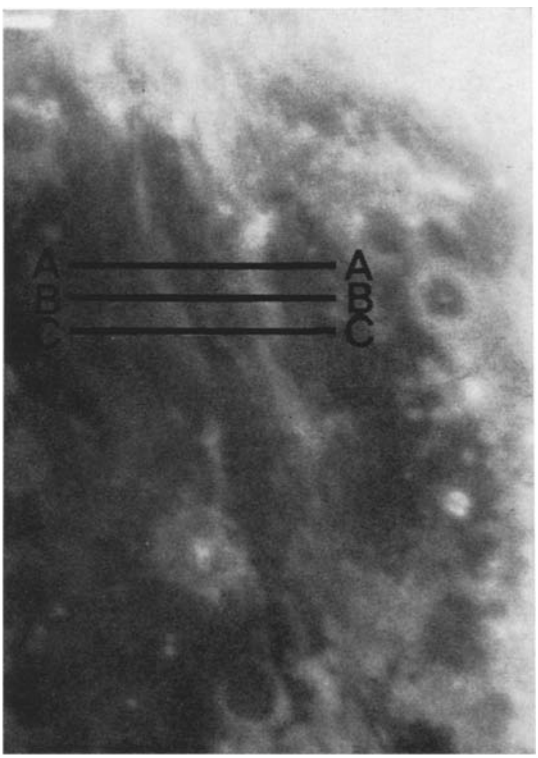

Fig. 3. Method of photometric measurement of the rays.

TABLE IV

Normal albedo (ϱ) of 7 rays of Kepler compared with the normal albedo of the background (ϱ_p), both $\times 10^3$. D = distance to the center of Kepler

Ray 1			Ray 2			Ray 3			Ray 4			Ray 7		
D (km)	ϱ	ϱ_p	D (km)	ϱ	ϱ_p	D (km)	ϱ	ϱ_p	D (km)	ϱ	ϱ_p	D (km)	ϱ	ϱ_p
55	145	110	65	140	110	80	122	119	55	145	110	35	155	110
70	110	105	85	110	105	165	101	83	70	110	105	45	150	110
90	103	82	105	88	82	200	103	84	90	105	82	55	152	110
110	106	83	130	118	83	260	88	82	110	105	83	70	152	110
135	108	81	155	106	82	285	99	89	135	101	81	80	147	110
160	103	88	180	101	89	310	85	83	165	103	89	90	137	110
190	98	83	205	100	83	335	91	88				105	132	110
210	98	88	230	103	88	360	93	87				115	129	110
230	94	87	255	99	87							125	129	110
			280	99	90							135	129	110
			300	99	85							150	121	110
			320	99	82							160	120	110
												170	116	110
												180	116	110
												190	116	110
												215	111	110
												230	110	110

Ray 5			Ray 6		
D (km)	ϱ	ϱ_p	D (km)	ϱ	ϱ_p
55	146	113	35	150	121
90	106	79	45	153	121
160	124	89	55	153	121
195	83	80	70	155	121
			80	156	121
			95	156	121
			105	150	121
			115	138	121
			125	129	121
			135	123	121
			150	121	121

In order to compare the rays with their surroundings, we selected the spacings AA, BB, ... so that they occupy also the undisturbed lunar surface on both sides of the ray.

The transmission in the centre of the ray was converted into intensity by the calibration curve of the plate. After multiplying it by a factor R in order to combine the measures of different plates, the normal albedo of the central part of the ray was found. The factor R defined in a previous paper (Van Diggelen, 1965) followed from a comparison with direct photoelectric measurements. In the same way the mean albedo of a number of points on both sides of the ray was determined for every section AA, BB, ...

From the diameter of the lunar image on the Yerkes plates (170 mm) we could calculate the distances D of the measured ray parts to the centre of the crater. In this way we have found a number of curves (Figures 4 and 8) showing how the albedo of the Moon varies along several rays. The same ray of Tycho has been measured on three different plates. The results show only a limited spread in the observed variation of the albedo. Therefore we have restricted the measurements of the other rays to only one plate.

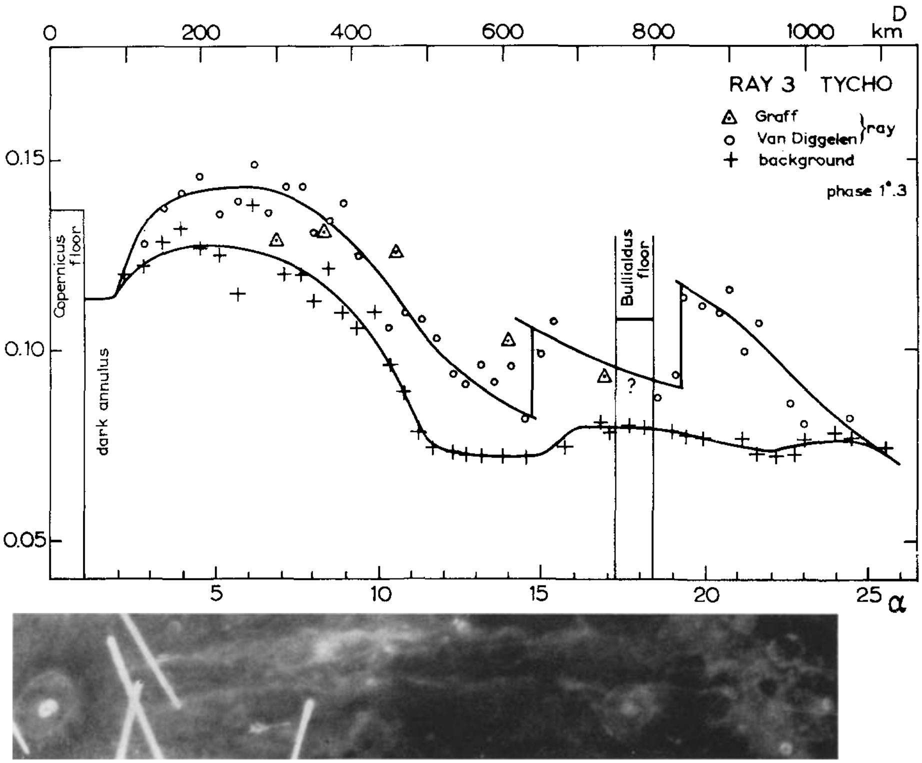

Fig. 4. Variation of the normal albedo along a Tycho ray and its surroundings.

3. Discussion of the Results

The margins of the rays observed from the Earth are diffuse, but the cause of this difference could not be determined from telescopic observations. The rays are composed of linear and feather-shaped elements and may be a texture of discrete, telescopically unresolved bright patches which are more widely spaced towards the ray margins (Lipsky and Shevchenko, 1968).

We assume that a fraction k of a unit area of a ray region is partly occupied by bright areas either juxtaposed or superposed, all these patches having the same area. If s is the area of such a bright patch and if n is their number per unit area, we may assume that

$$k = 1 - \exp(-ns). \tag{1}$$

The fraction of the area between the patches of the unit area is given by

$$1 - k = \exp(-ns). \tag{2}$$

From such a unit area we shall observe a normal albedo

$$\varrho = k\varrho_s + (1-k)\,\varrho_p = k(\varrho_s - \varrho_p) + \varrho_p, \tag{3}$$

where ϱ_s = the normal albedo of the unknown white material surrounding bright craters, and ϱ_p = the normal albedo of the undisturbed background.

The quantity ϱ_p has been observed and tabulated for all the measured rays. For ϱ_s we can assume a reasonable value. This value is approximated by assuming $n \to \infty$ in which case $k \to 1$, so that $\varrho = \varrho_s$ the maximal value of ϱ observed. From ϱ, ϱ_p and ϱ_s we have determined the fraction k of the unit area occupied by bright patches (Table V). Figure 5 shows how this fraction varies with the distance D to the centre of the crater for one of Tycho's rays.

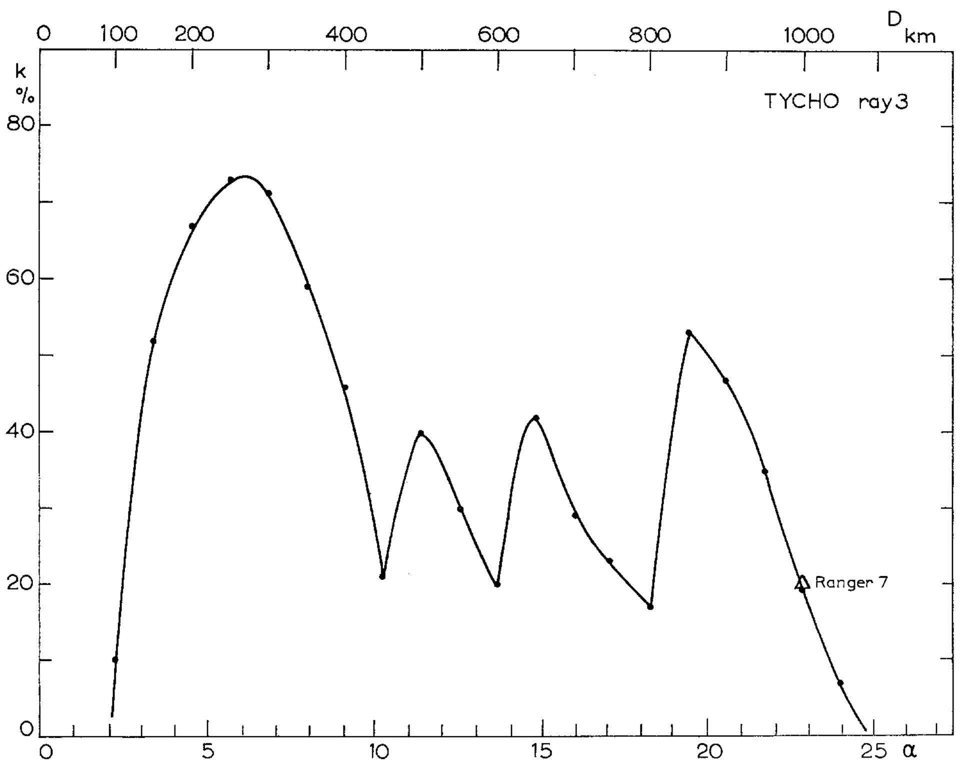

Fig. 5. Variation of the percentage k of a unit area of a ray occupied by bright patches.

TABLE V
The k-values of the observed rays

D (km)	Rays of Tycho					Rays of Copernicus													Rays of Aristarchus					Rays of Kepler						
	1	2	3	4	5	1	2	3	4	5	6	7	8	9	10	11	12	13	1	2	3	4	5	1	2	3	4	5	6	7
50																				75				69	58	36	70	80	87	
100	47	29	10		47												59	64		43	75	36		19	56	26	24	54	82	
150	46	61	52		67			66									49	46	52	43	54	40	26	16	39	22	21	30	0	
200	43	67	67	84	84	0	19	42	50			15	56	78		77	36	29	38	27	29	40	29	12	26	17		6		
250	42	73	73	88	99	61	28	20	48	7	26	39	70	67		48	24	11	26			22	26	8	12	13				
300	44	78	71	39	88	41	18	58	48	27	39	45	46	57	48	33	10	0	18							8				
350	43	79	59	30	73	39	9	49	48	38	46	43	37	51	37	24	0									5				
400	44	79	46	19	59	33		43	36	31	38	34	29	51	25															
450	42	72	21	5	52	24		37	24	23	29	26	35	40	20															
500	40	59	40	35	44	61		30	13	16	22	19	41	17																
550	40	46	30	35	47	33		16			14	11	47	6																
600	33	36	20	34	35	67																								
650	31	29	42	34	27	26																								
700	28	23	29	36	69																									
750	28	22	23		65																									
800	26	21	17	36	61																									
850	27	55	53		55																									
900	25	43	47	36	48																									
950		34	35		40																									
1000		27	19	33	37																									
1050		22	7	30	26																									
1100				21	22																									
1150				17	22																									
1200				20	19																									
1250					11																									
1300				29																										
1400				80																										
1450				16	78																									
1500				53	78																									
1550					44																									
1600				38	34																									
1650					22																									
1700				65	11																									
1750					4																									
1800				26																										
1900				7																										
2000				8																										
2100				9																										

We have counted in frame 196 (Ranger 7 photographs of the Moon, Part I, A camera frames) in a unit area of 4×4 km^2 the total area occupied by bright patches of different sizes. The measured area is centered around $\beta = -10°.70$, $\lambda = -20°.78$, i.e. 1000 km from the centre of Tycho. We have found here the value $k = 19.5\%$ in accordance with our photometric curve (Figure 5). We may thus assume that the distribution of ϱ along a ray is determined by the fractional area covered by the unresolved bright patches along that ray which can only be analysed by spacecraft photographs.

It is not certain, however, that the bright rays are only caused by bright telescopically unresolvable patches. The high-resolution photographs obtained by Ranger 7 (Shoemaker, 1966) have revealed that the bright walls of some of the ray-craterlets contribute to the brightness, but that this effect is superimposed on a background of more uniform albedo between the bright-walled craterlets. This background albedo diminishes according to Shoemaker gradually toward the ray margin. Over distances of a few meters, areas in a Tycho ray appear to be nearly uniform in albedo. The bright material is probably derived from the nearest craterlets, although fragments from other secondaries within the ray and from the primary crater are also present. The difference in albedo shown by the ray material is probably related to differences in mineral or chemical composition, as stated by the Surveyor 7 results.

We have assumed that the albedo between the bright patches is the same as the albedo besides the rays. If this supposition is not correct it cannot have much influence on the results of k. Exact photometric results of the Ranger photographs have not been published, and the counted number in frame 196 proves that our theoretical interpretation is in broad outline justified.

4. Comparison with the Rays of Terrestrial Explosion Craters

Rayed patterns have been observed on Earth also around chemical and nuclear craters. The distribution of the ejecta with respect to the explosion epicentre has been studied for several events (Carlson and Jones, 1965). Crater ejecta appear to be deposited in longitudinal mounds radially oriented in the regions adjacent to the crater. Rays sometimes appear to be tangential rather than radial with respect to the crater. The same phenomena have been found for the lunar rays of Copernicus.

The experimental values of the areal density of the ejecta can mathematically be approximated by functions of the form

$$\delta = CD^b, \tag{4}$$

where δ = the areal density in g/m^2; C = a proportionality constant; D = the distance from the epicentre in m, and b = decay constant for the ejecta. If we take $\alpha = D/R$, where R = the radius of the crater in m, we get

$$\delta = C'\alpha^b. \tag{5}$$

A new discussion of the figures with the observed points of Carlson and Jones gives

TABLE VIA

b and $\log C'$ for terrestrial explosion craters (Carlson and Jones, 1965)

creater	R	b	$\log C'$
He-2	11.7	−3.4	4.07
Scooter	46.9	−5.3	5.45
Stagecoach 2	15.4	−2.3	2.54
Stagecoach 3	17.9	−2.7	4.47
Suffield	21.3	−2.9	3.79
Sedan	182.9	−3.6	1.33
Teapot Ess	44.5	−3.4	6.14

TABLE VIB

Height of the ejecta in cm, assuming a lunar surface density = 3 for different values of C'

α	$C' = 10^5$	10^4	10^3	10^2	10
2	2930	293	29.3	2.930	0.293
4	259	25.9	2.59	0.259	0.026
6	63	6.3	0.63	0.063	0.006
8	23	2.3	0.23	0.023	0.002
10	11	1.1	0.11	0.011	0.001
12	6	0.6	0.06	0.006	0.001
14	3.3	0.33	0.033	0.003	
16	2.0	0.20	0.020	0.002	
18	1.1	0.11	0.011	0.001	
20	1.0	0.10	0.010	0.001	
22	0.7	0.07	0.007	0.001	
24	0.5	0.05	0.005	0.001	
26	0.4	0.04	0.004		
28	0.3	0.03	0.003		
30	0.2	0.02	0.002		

the values for b and C' listed in Table VI. It appears that we may assume that

$$\delta = C'\alpha^{-3.5}, \tag{6}$$

where C' varies form 10 to 10^6.

There can be significant variations in the quantities of ejected material measured at a constant α for terrestrial craters. The variation in C' by a factor 10^5 for a constant α gives a satisfying interpretation of the observed rays. We assume, however, that the value of C' is constant along a ray. If we assume also that the density of the ejecta does not vary significantly along the ray, we have found now not only the variation of δ with α, but also the variation of the height of the layer of ejecta with the distance to the epicentre.

We have just seen that the lunar rays can be interpreted as samples of telescopically unresolved bright patches. Many astrononers, however, have supposed that the rays would be regions covered with powdery matter ejected form the central crater and uniformly spread over the surface. If we assume that formula (6) may be used, we can compare this old hypothesis with our photometric results. From Table VIB we can try to find a value for C'. The lunar rays extend for several hundreds of km. If we plot, however, their length as a function of α (Figure 4), we can compare first this length directly with the terrestrial results. Their mean length varies between 12 and 28 (Table VII), and from Table VIB we see that C' between 10^3 and 10^5 gives a very good approximation for such cases, if we assume that the rays end as soon as the height of the ejecta may be ≤ 0.05 cm.

TABLE VII

Length of the rays α expressed in the crater radius R

nr. of Ray	Tycho	Copernicus	Aristarchus	Kepler
1	21	16	17	14
2	25	8	13	20
3	25	14	20	22
4	42	14	19	10
5	41	13	20	14
6		13		12
7		14		9
8		13		
9		14		
10		11		
11		8		
12		8		
13		7		
mean value	31	12	18	14
R (in km)	44	41	20	16
mean ray (in km)	1365	490	360	224

If the lunar rays are composed of a *homogeneous layer of fine debris* ejected from the crater, we can get an idea about the height of the layer. Optical and infrared measurements indicate that the lower bound in the prevalent particle size on the surface of the Moon is 10 μ. Gehrels' (1960) measures of polarization suggest surface particle sizes smaller than 0.3 μ. Measurements of microwave radiation predict an upper bound between 300 and 1000 μ (Fensler *et al.*, 1962). If we assume with the Surveyor results 0.1 mm for the particle size, we may indeed expect that the brightness of layers of a height of 0.5 mm or more is independent on its depths. As 0.1 mm is near the upper limit of the size for these bright particles, we may certainly assume their brightness not to depend much on the height of the layer. Now we can conclude from Table III that $C'=10^4$ gives the best approximation. Values for $C'=10^5$ can still be accepted though the height of the layer in the direct surroundings of the crater is now already about 100 m.

There are, however, important arguments for assuming our original hypothesis that the rays are composed of a number of bright patches and not uniformly covered with a bright powder. The albedo of the rays is not constant, but their brightness behaves in the same way as the region through which they pass. They are darkened on a Mare region and brighter on continental background. If we neglect the great irregular variations and reduce the normal albedo to its value on a more uniform background, we can clearly see that the albedo diminishes slowly along the ray from the central crater outwards. This can be understood as a slow diminishing of the fractional area covered by unresolved bright patches. Values for $C' = 10^4$ or 10^5 give a height of a uniform layer of material of many meters and extending over large areas. Such a thick layer would have been detected through modern photographic investigations by space vehicles. If the ejecta have not covered the ray regions uniformly, it may still be possible to compare the areal density of the matter with the terrestrial explosion craters, but we now get a greater height for the layer on those patches, where the powdery matter has fallen. Such a height does not seem to be in accordance with the observations. It might be possible that the distributions must now be approximated by another function as the formula (6), but it can also be assumed that the rays originated by another process.

Kopal (1966) has already given strong arguments for the theory that depressions on Tycho's rays are due to subsidence rather than to impact. It may also be possible that the rays are caused by the seismic quake which shook the Moon when the central crater originated. In those regions, where the lunar surface was strongly triggered by the seismic quake the material might have come into a state of lower porosity. The albedo of the lunar surface may be strongly dependent on the porosity of the material as has been found from the footprints of the Surveyor 1 (Halajian, 1968).

5. Interpretation of the Rays

We have measured 5 rays of the Tycho system. Comparison with the measurements of Graff (1948) shows a good accordance. Rays 2 and 3 of Tycho cross the Mare Nubium. The albedo of these rays diminishes steeply in agreement with the general darkening of the background. The coincidence of the photometric properties of the rays and those of the background proves that the rays cannot be composed of a thick homogeneous layer of ejected powdery matter. The Ranger 7 photographs had also suggested that this simple theory could not be right for the interpretation of the fine structure of the rays. The comparison with the terrestrial explosion craters is also in accordance with this behaviour. The same effect is also observed for ray 5 of Tycho when it crosses the Mare Nectaris. The ray seems to have its end on Mare Foecunditatis. Ray 4 gives the impression to end at about $\alpha = 42$. The ray on Mare Serenitatis in the same direction may belong to Menelaos.

Tycho is the crater with the greatest ray system. Near the crater itself we observe a dark halo, from which the boundaries have already been determined by Fielder (1961). Its albedo is about $0^m.02$ less that that of the crater floor. Fielder found that the rays 2 and 3 do not intrude into the halo, as has now been confirmed photometrically. The reality of the halo, which shows clearly on the proper photographs (Figure 6), has been proved. Its origin may be the heat originated by the Tycho explosion. Another

Fig. 6. The relatively dark aureole surrounding Tyche (120-inch reflector of Lick, reproduced from Z. Kopal, *An Introduction to the Study of the Moon*, 1966, p. 248).

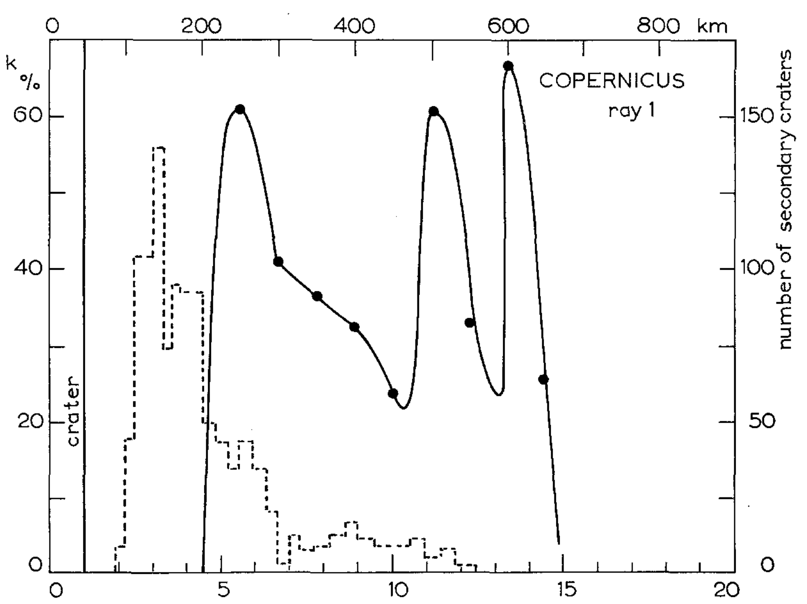

Fig. 7. The distribution of secondary craters of Copernicus (dashed) compared with the distribution of the k-values (solid lines).

explanation may be that the halo is composed of dark ejected powdery matter with less porosity than other regions.

The albedo along the rays diminishes slightly and does not show a maximum at $\alpha = 12$. There are pronounced variations showing that the rays are composed of a number of *ray segments*. The same effect is shown by plotting the fractional area k covered by bright spots in the same region. The k-distribution curves (Figure 5) show the same ray segments.

We have compared the distribution of k of the rays of Copernicus (Figure 7) with the distribution of the secondary craters around the primary, as has been counted by Shoemaker (1962), but the ray segments do not appear to be situated at the same distance from the central crater as the secondary craters.

Fielder (1965) suggests that the rays are pre-melt for some maria and post-melt for others. The rays of Proclus are clearly visible in Mare Crisium, but they are absent in Mare Tranquillitatis. Our investigation shows that the rays of Kepler shows a sharp fall in albedo beyond $\alpha = 5$. There are indications that the albedo slightly increases (about $0^m.008$) form $\alpha = 2$ to $\alpha = 5$. So there is an indication of a darker halo around

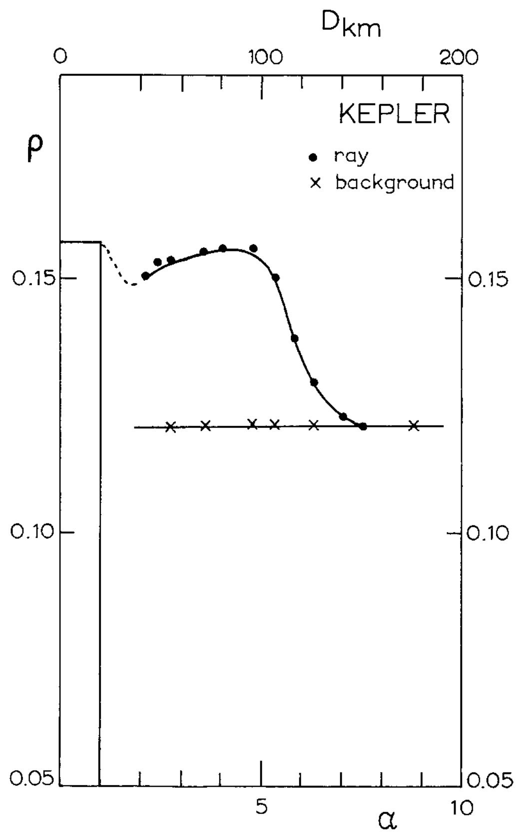

Fig. 8. Variation of the normal albedo along a Kepler ray showing traces of the existence of a dark aureole.

this bright crater, but at $\alpha = 5$ the albedo is again as high as in the center of Kepler. As this whole region is about $0^m.07$ brighter as compared with the Oceanus Procellarum surrounding it, we cannot see clearly the outlines of the faint halo. Kepler must be a post-melt object.

Acknowledgements

It is a pleasure to acknowledge helpful discussion with Professor M. Minnaert, who offered a number of valuable suggestions. I wish to thank M. J. Degewij for measuring the plates during his stay at the Utrecht Observatory.

References

Carlson, R. H. and Jones, G. D.: 1965, *J. Geophys. Res.* **70**, 1897.
Fensler, W. E., Knott, E. F., Olte, A., and Siegel, K. M.: 1962, in *The Moon* (ed. by Z. Kopal and Z. K. Mikhailov), Academic Press, New York, p. 545.
Fielder, G.: 1961, *Astrophys.* J. **134**, 425.
Fielder, G.: 1965, *Lunar Geology*, Butterworth Press, London.
Gehrels, T.: 1960, *Lowell Obs. Bull.* **4**, 300.
Graff, K.: 1948, *Sitzber. Öster. Akad. Wiss.*, Abt. IIa **157**, 17.
Halajian, J. D.: 1968, Report no SAS 425-5, Grumman Aircraft Eng. Corp., New York.
Kopal, Z.: 1966, *Icarus* **5**, 201.
Lipsky, Y. N. and Shevchenko, V. V.: 1968, *Astron. Zh.* **45**, 389.
Radlova, R. N.: 1943, *Astron. Zh.* **20**, 1.
Shoemaker, E. M.; 1962, in *Physics and Astronomy of the Moon* (ed. by Z. Kopal), Academic Press, New York and London, p. 283.
Shoemaker, E. M.: 1966 in *The Nature of the Lunar Surface* (ed. by W. N. Hess, D. H. Menzel, and J. A. O'Keefe), Johns Hopkins Press, Baltimore, p. 23.
Van Diggelen, J.: 1965, *Planetary Space Sci.* **13**, 271.